Proceedings of FEDSM2005
2005 ASME Fluids Engineering Division Summer Meeting and Exhibition
June 19-23, 2005, Houston, TX, USA

FEDSM2005-77175

VORTEX DYNAMICS AND MECHANISMS FOR VISCOUS LOSSES IN THE TIP-CLEARANCE FLOW

Donghyun You*, Meng Wang, and Parviz Moin
Center for Turbulence Research
Stanford University
Stanford, California 94305

Rajat Mittal
Department of Mechanical and Aerospace Engineering
George Washington University
Washington, District of Columbia 20052

ABSTRACT

The tip-clearance flow in axial turbomachines is studied using large-eddy simulation with particular emphasis on understanding the underlying mechanisms for viscous losses in the end-wall region and the unsteady characteristics of the tip-leakage vortical structures. Systematic and detailed analysis of the mean flow field and turbulence statistics has been made in a linear cascade with a moving end-wall. The tip-leakage jet and tip-leakage vortex are found to produce significant mean velocity gradients, leading to the production of vorticity and turbulent kinetic energy. These are the major causes for viscous losses in the cascade end-wall region. An analysis of the energy spectra and space-time correlations of the velocity fluctuations suggests that the tip-leakage vortex is subject to a pitchwise low frequency wandering motion.

NOMENCLATURE

C	Chord length
C_a	Axial chord length
f	Frequency
p	Pressure
Re	Reynolds number
t	Time
U	Time-averaged streamwise velocity
U_∞	Inflow freestream velocity
u_i	x_i component of velocity
u	Streamwise velocity
u_τ	Friction velocity
V_{belt}	End-wall velocity
v	Cross-stream velocity
w	Vertical velocity
x_i	Cartesian coordinates
x	Streamwise coordinate
y	Cross-stream coordinate
z	Vertical coordinate
ν	Kinematic viscosity
Δ	Grid spacing
$()^+$	Quantity in wall-unit
$()'$	Fluctuation component

INTRODUCTION

The radial clearance between a rotor-blade tip and casing wall in a turbomachine is indispensable for its operation. However, its existence has been a major source of unfavorable flow phenomena. Complicated vortical structures are generated by the tip-clearance flow and its interactions with the end-wall boundary layer, the blade wake, and neighboring blade. The tip-clearance vortical structures often induce rotating instabilities and blockage in the flow passage which result in severe performance loss and subsequent stall of axial compressors [1,2]. Also, in a transonic compressor, interaction between passage shock and tip-clearance flow is implicated in the degradation of efficiency as well as vibrations and noise generation [3]. These issues have motivated a number of experimental and computational inves-

*Corresponding author. Email: dyou@stanford.edu

tigations of the compressor tip-clearance flow, and some basic understanding has been achieved (see e.g. [4–11]).

On the other hand, in hydraulic turbomachines such as submarine propulsors and liquid pumps, the existence of tip clearance is considered to be a cause for cavitation, which can result in loud acoustic noise, performance deterioration, and the erosion of blades and casing wall (see e.g. [8, 9, 12–14]). In order to understand the mechanisms for cavitation, it is necessary to study the detailed turbulence and vortex dynamics in the rotor-blade wake and tip-clearance region and the associated low pressure events.

In the most recent experiments performed by Devenport's and Simpson's groups at VPI [15–18], low speed linear compressor cascades with stationary and moving end wall were employed. Mean velocity, vorticity, turbulent kinetic energy, and frequency energy spectra have been measured downstream of the rotor blades for tip gaps of 0.83%, 1.65%, and 3.3% chord. Wang and Devenport [16] employed a moving end wall and found noticeable difference in the mean velocity and Reynolds stress distributions from the experiments which utilized a stationary end wall [15]. Kuhl [17] and Ma [18] examined the effects of upstream vortex pairs on the downstream tip-leakage vortex. Employing a stationary end wall, Wenger *et al.* [19] performed two-point measurements of the turbulent fluctuations in the downstream tip-leakage flow, and showed conclusively that the tip-leakage vortex is not subject to low-frequency pitchwise "wandering" motions. On the other hand, an experiment employing a moving end wall [16] showed a noticeable low-frequency spectral peak in the pitchwise velocity energy spectra which is quite different from the peak in the blade wake. However, no further investigation regarding the origin and mechanism of this low-frequency peak were made.

These experiments [15–18] have provided useful information regarding the flow as well as valuable data for validating computational techniques. However, since the measurements were limited to the flow field at least one and half chord lengths downstream from the trailing edge, they could not shed light on the upstream flow features which are critically important.

Experimental measurements of the tip-leakage flow in the vicinity of the tip gap very close to the end wall are generally difficult due to technical and safety issues. In addition, the strong unsteadiness of the tip-leakage flow limits the applicability of conventional Reynolds-averaged Navier-Stokes (RANS) approaches in a computational study. These difficulties have been major obstacles to a detailed understanding of the tip-leakage flow physics leading to viscous losses. Although, the gross feature of the tip-leakage vortex has been known for some time, a deeper quantitative understanding of the dynamics of the tip-leakage vortical structures and their interaction with the end-wall boundary layer is needed to elucidate the viscous loss mechanisms.

In this study, the tip-leakage flow, particularly in regions not studied experimentally, is investigated using data generated by large-eddy simulation (LES). The objective is to gain an improved understanding of the mechanisms for viscous losses associated with the tip-leakage flow in turbomachines and the unsteady characteristics of the vortical structures. In order to gain such an understanding, it is necessary to study the detailed turbulence dynamics in the rotor-blade wake and the tip-clearance region and to examine the space-time correlations of the coherent turbulence structures present in the end-wall tip-leakage flow.

Furthermore, a detailed investigation regarding mean pressure and pressure fluctuations has been carried out, which helps understand tip-leakage cavitation in hydraulic turbomachines. The results will be presented in a future publication.

COMPUTATIONAL METHODOLOGY

Numerical Method

The numerical algorithm and solution method are described in detail in Ref. [20]. Here, we summarize the main features of the methodology.

The three-dimensional, unsteady, incompressible Navier-Stokes equations are solved in a generalized coordinate system in conjunction with a Smagorinsky type dynamic subgrid-scale (SGS) model. Given the fully inhomogeneous nature of the flow, a Lagrangian dynamic SGS model, which averages the model coefficient along the flow pathlines [21], is employed.

The integration method used to solve the governing equations is based on a fully-implicit fractional-step method which avoids the severe time-step restriction in the tip-clearance region. All terms including cross-derivative diffusion terms are advanced in time using the Crank-Nicolson method and are discretized in space by energy-conserving second-order central-differencing. A Newton iterative method is used to solve the discretized nonlinear equations. For the pressure Poisson equation, an efficient multigrid procedure, which is a combination of the line and red-black Gauss-Seidel multigrid method is used. This method is particularly appropriate for parallelization. The simulation code is parallelized using OpenMP.

Computational Setup

The flow configuration and coordinate definition are schematically shown in Fig. 1. The present study is focused on a linear cascade with a moving end-wall at the bottom of the tip gap that matches the experimental setup of Wang and Devenport [16]. Only a single blade is considered, with periodic boundary conditions in the y-direction to mimic the flow in the interior of a cascade. The computational domain is of size $L_x \times L_y \times L_z = 1.8C \times 0.929C \times 0.5C$, where C is the blade chord. The mesh size used for the final simulation is $449 \times 351 \times 129$.

The important parameters for the base simulation are as follows: The size of the tip clearance is $0.0165C$, the blade pitch is

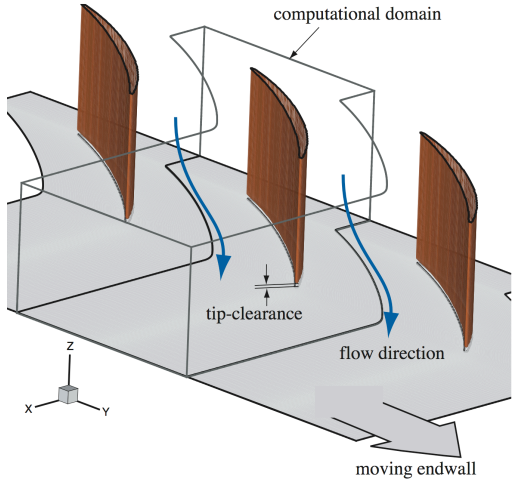

(*a*)

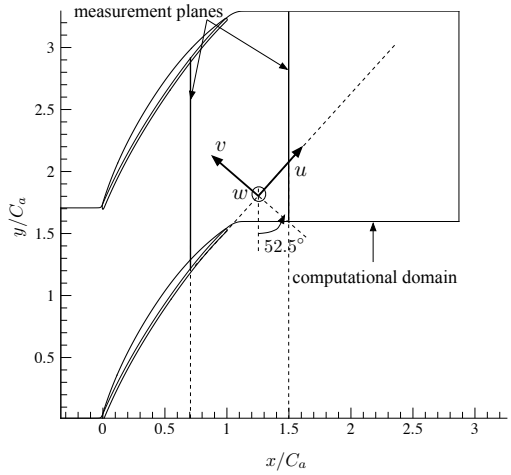

(*b*)

Figure 1. Flow configuration and coordinate system. (*a*) Three-dimensional view; (*b*) top view showing planes for detailed analysis.

$0.9C$, and the blade span is $0.5C$ ($1C$ in the experiments). The blade has a relatively high stagger-angle of about 57 degrees. The Reynolds number of this flow is $400,000$ based on the chord and inflow free-stream velocity, and the inflow turbulent boundary layer has a Reynolds number of 780 based on the momentum thickness.

The inflow turbulent boundary-layer data is provided using the method of Lund *et al.* [22], modified to account for the fact that the mean flow direction is not perpendicular to the inflow/outflow plane. No-slip boundary conditions are applied along the rotor blade and moving end wall, and convective boundary condition is applied at the exit boundary.

The difficulty with grid topology in the tip-clearance region is overcome by a novel approach which combines an immersed boundary technique [23] with a structured grid in a generalized coordinate system. In addition to this, the high stagger angle in the experimental setup necessitates the use of very skewed mesh, which requires fine control of mesh parameters such as stretching ratio and aspect ratio, and an adequate formulation of nonlinear convection terms to avoid numerical instability (see Ref. [24] for more details).

The grid spacing and resolution in wall units in the important regions are reported in Ref. [24] in detail. In general, the grid resolution on the blade surface is reasonable compared to previous LES studies of wall bounded turbulent flows using similar numerical methods [25]. Grid resolution normal to the end wall ($0.3 \leq \Delta z^+ \leq 2.1$) is also reasonable. In the directions parallel to the end wall, Δx^+ and Δy^+ are generally less than 50, except in a small end-wall region where the maximum values reach $90 \sim 100$ because of the strong effect of the tip-leakage vortex on the boundary layer. The present mesh is determined iteratively based on the results from a number of coarser-mesh simulations.

The simulation is advanced in time with the maximum Courant-Friedrichs-Lewy (CFL) number equal to 4 which corresponds to $\Delta t U_\infty / C \approx 0.73 \times 10^{-3}$ where U_∞ is the incoming freestream velocity. Each time-step requires a wallclock time of about 900 seconds when 32 CPUs of an SGI Origin 3800 are used. In wall units, the time-step is in the range of $0.078 \leq \Delta t^+ = \Delta t u_\tau^2 / \nu \leq 3.79$. The maximum Δt^+ is found underneath the blade tip, and except for this location, Δt^+ is generally less than 0.8. The results which will be discussed below are obtained by integrating the governing equations over a time interval of about $20C/U_\infty$.

A systematic validation of the LES predictions has been conducted and reported in [20, 24]. Comparisons are made with experimental data [16] in terms of mean velocity and turbulence statistics in the measurement planes downstream of the trailing edge, and reasonable agreements are obtained.

RESULTS AND DISCUSSION

Overall features of the tip-clearance flow

Gross features of the end-wall vortical structures found in the present study are visualized using the λ_2 vortex identification method [26] and shown in Fig. 2. In this vortex identification method, eigenvalues of the symmetric tensor $S^2 + \Omega^2$, where S and Ω are respectively the symmetric and antisymmetric parts of the velocity gradient tensor, are considered. If λ_1, λ_2, and λ_3 are the eigenvalues and $\lambda_1 \geq \lambda_2 \geq \lambda_3$, the definition of a vortex in an incompressible flow is equivalent to the requirement that $\lambda_2 < 0$ within the cortex core. The most dominant vortical structure is the tip-leakage vortex which originates at about 20% to 30% of the axial chord downstream from the leading edge. This vortex and tip-separation under the blade tip near the leading edge

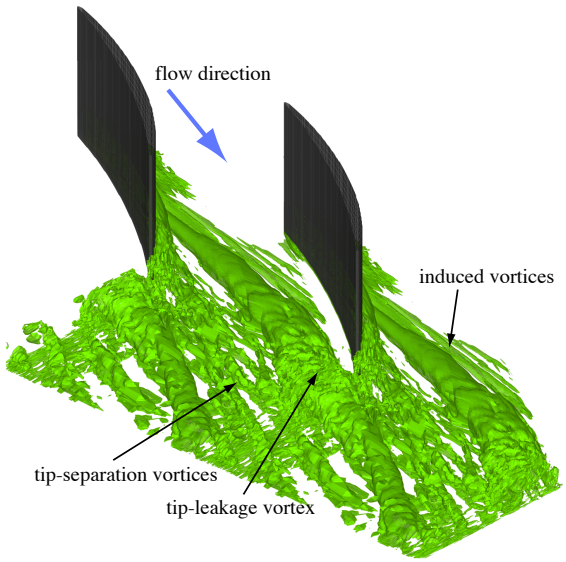

Figure 2. λ_2 iso-surfaces from time-averaged flow field.

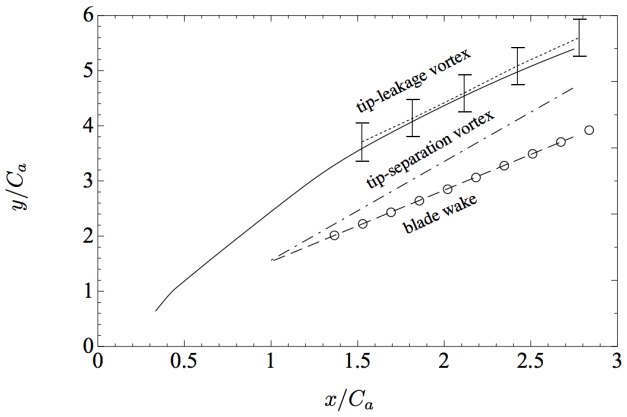

Figure 3. Trajectories of tip-leakage vortex core, the dominant tip-separation vortex and the center of blade wake projected onto the end-wall plane. ——— , – – – – , —·— , present LES; ···⌶··· , ○ , experiment [16].

generate induced vortices. Highly unsteady vortical motions are found in the trailing edge region. In this region, tip-separation vortices become highly complicated due to the interaction with the tip-leakage vortex and blade wake. Similar observations have been reported by other experimental and numerical studies in tip-clearance configurations [15, 16].

Trajectories of the tip-leakage vortex core, the dominant tip-separation vortex, and blade wake are compared in Fig. 3 with experimental measurements [16]. The core of the tip-leakage vortex is defined as the point of maximum streamwise vorticity through the tip-leakage vortex similar to that in the experiment [16]. The dominant tip-separation vortex is found using the λ_2 vortex identification method and the core of the λ_2 contour is used to determine its trajectory. To describe the trajectory of the blade wake, locations of peak streamwise velocity deficits at $z/C_a = 0.9$ are traced.

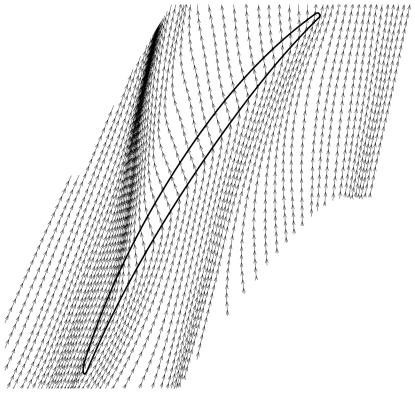

Figure 4. Streamlines of mean velocity field in an $x-y$ plane at $z/C_a = 0.025$.

The trajectories of the tip-leakage vortex and blade wake are in good agreement with experimental data in the wake region, also shown in the Fig. 3. However, details regarding the tip-separation vortices were not clearly identified in the experimental study. This may be due to high-speed motion of the end wall hindering measurements of flow quantities near the end wall.

The trajectories of the tip-leakage vortex in the cascade passage region ($x/C_a \leq 1$) and tip-separation vortex downstream of the trailing edge show larger propagation angles with the streamwise coordinate compared to those found in the rest of the tip-leakage vortex and the blade wake. Since the tip-leakage vortex in the cascade passage and the downstream tip-separation vortices are located close to the end wall, their positions are strongly affected by the end-wall motion in the positive pitchwise direction. Downstream of the trailing edge, the tip-leakage vortex is lifted from the end wall. Its trajectory and the trajectory of the blade wake are hence aligned with the cascade main stream.

The pressure difference between the pressure and suction sides of the blade tip and the moving end wall drive the tip-leakage flow across the tip gap. The streamlines in an $x-y$ plane close to the end wall are shown in Fig. 4, which reveal the driving mechanism for tip-leakage flow. A convergence of the streamlines along the locus of the tip-leakage vortex is observed. The tip-gap flow experiences a sudden change of flow direction across the converging streamlines. Upstream of the converging streamlines, the flow direction is approximately aligned with the blade chord, while the flow direction is altered to the positive pitchwise direction in the region between the tip-leakage vortex

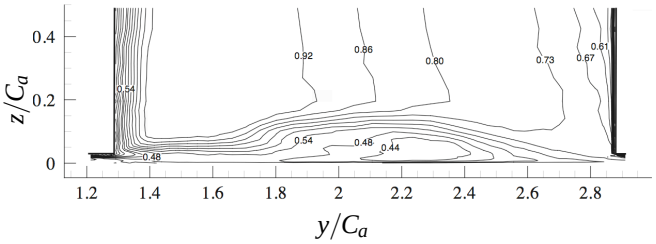

Figure 5. Contour plot of mean streamwise velocity component in a $y-z$ plane at $x/C_a = 0.7$.

and the blade suction surface. As a result of flow turning, the streamwise velocity component is significantly reduced in this region as shown in Fig. 5.

Although an accurate prediction of the flow field underneath the blade tip is crucial for understanding the vortical structures and their generation and evolution mechanisms, in previous studies, numerical prediction of these flow features has been difficult due to the issues with grid topology and grid resolution in the tip-gap region. Oil or paint film visualization techniques have been the most common way of experimentally investigating the flow field inside the tip gap.

Mean Flow Field and Turbulence Statistics

In this section, the mean flow field and turbulence statistics in the cascade passage, where the tip-leakage and tip-separation vortices and induced vortices are generated and evolve, are discussed. The analysis complements the experimental study of Wang and Devenport [16] in which no measurement was made inside the blade passage. Furthermore, it allows a study of the flow to a level of detail not accessible by experimental resolution.

In the cascade passage, the tip-leakage jet, driven by the pressure difference between the pressure and suction sides of the blade tip, plays an important role in the vorticity and turbulence production. The tip-leakage jet is found to produce significant mean velocity gradients ($\partial U/\partial z$) due to the direction change of the flow along the spanwise direction as shown in Fig. 5, which shows the mean streamwise velocity component in a $y-z$ plane at $x/C_a = 0.7$ from the view-point of an observer looking upstream (left- and right-hand side walls represent the suction and pressure surfaces of two neighboring blades, respectively).

The tip-leakage vortex approaches the pressure side of the neighboring blade with increasing chord-wise coordinate. As the flow passes through the cascade passage, it is observed that the magnitudes of the streamwise velocity in the cascade core region and the pitchwise velocity near the end wall are rapidly reduced (see Ref. [24] for more details). This is a desired transition of dynamic head to static pressure rise in axial compressors or pumps.

The significant mean velocity gradients also results in enhanced vorticity magnitudes. Figure 6 shows the contour plots of three mean vorticity components in a $y-z$ plane at $x/C_a = 0.7$. In the end-wall region, the streamwise ($\Omega_x C/U_\infty$) and pitchwise ($\Omega_y C/U_\infty$) vorticity components dominate the vorticity field and this suggests that the tip-leakage vortex evolves in a helical configuration. The jet-like leakage flow underneath the blade tip produces higher vorticity levels in the streamwise and pitchwise components compared to that in the tip-leakage vortex. Large spanwise vorticity ($\Omega_z C/U_\infty$) is observed on the blade pressure and suction surfaces due to the boundary layers.

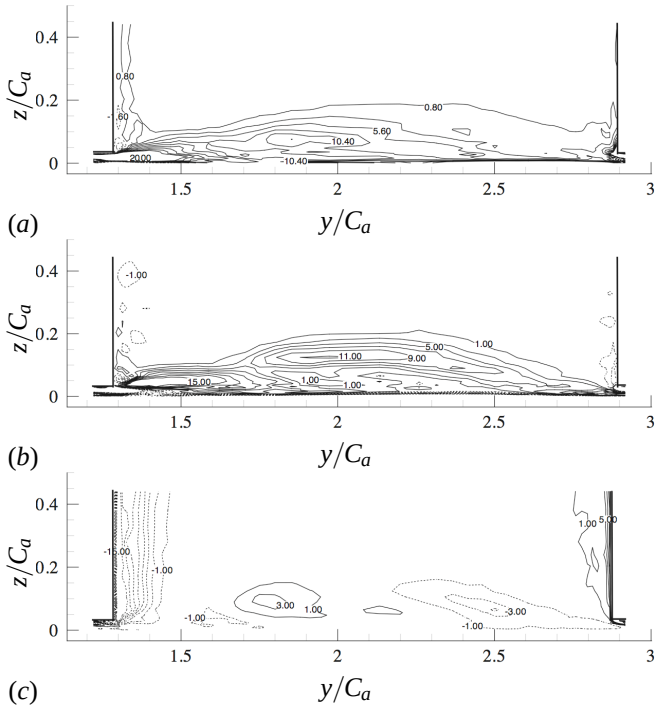

Figure 6. Contour plots of mean vorticity components in a $y-z$ plane at $x/C_a = 0.7$. (*a*) $\Omega_x C_a/U_\infty$; (*b*) $\Omega_y C_a/U_\infty$; (*c*) $\Omega_z C_a/U_\infty$.16 contour levels are shown in the ranges of ± 20, ± 15, and ± 15, for (*a*), (*b*), and (*c*), respectively. Dashed lines indicate negative values.

In general, in the blade passage, the regions of tip-leakage, blade-tip, and blade boundary layer generate strong vorticity magnitudes. Among them, the vorticity magnitude underneath the blade tip overwhelms the magnitudes found in the tip-leakage vortex and separated blade boundary layer. The latter two regions have comparable vorticity magnitudes. In the tip-leakage vortex, the location of peak streamwise vorticity corresponds to the vortex core. The peak vorticity magnitude in the tip-leakage vortex decays as it develops downstream. In addition, as also noticed in Wang and Devenport's [16] experiments, the tip-leakage vortex in the blade wake decays rapidly with the streamwise coordinate.

A region of high pitchwise vorticity is found between the tip-leakage vortex and the suction side of the blade tip (Fig. 6(*b*)).

Intense negative pitchwise vorticity is found along the jet-like flow near the end wall, and this is closely related to the direction of tip-leakage flow. As shown in Fig. 4, the end-wall leakage flow, which is directed upstream by the pressure difference between two sides of the blade tip and the end-wall motion along the positive pitchwise direction, generates strong negative pitchwise vorticity ($\Omega_y = 1/2(\partial U/\partial z - \partial W/\partial x) \approx \partial U/\partial z < 0$). On the contrary, significant levels of positive pitchwise vorticity are produced in the adjacent upper region where the leakage flow and cascade core flow generate large positive spanwise derivatives of the streamwise velocity ($\partial U/\partial z > 0$).

A vortex generator can be utilized to diminish the strength of the tip-leakage vortex. Kuhl [17] and Ma [18] examined the effects of an upstream counter-rotating vortex pair produced by a vortex generator on the tip-leakage vortex. They observed significant modification of the downstream tip-leakage flow field. However, since the streamwise vorticity field (Fig. 6(a)) mainly consists of counter-clockwise rotating vortices (from the viewpoint of an observer looking upstream), it would seem more desirable to employ upstream clockwise co-rotating vortices instead of the counter-rotating vortex pair. In order to control the pitchwise vorticity (Fig. 6(b)), which is quite significant in the tip-leakage jet region, shape modification of the blade cross-sectional profile and blade tip seems to be more appropriate since the direction and magnitude of the pressure gradient across the blade tip is the major source of the vorticity.

The tip-leakage vortex, tip-leakage jet, and blade boundary layer separation generate strong turbulent fluctuations. To examine this, the transport equation for the Reynolds normal stresses or turbulent kinetic energy k, is expressed as:

$$\frac{Dk}{Dt} = \wp + T + \varepsilon, \tag{1}$$

where

$$\begin{aligned} k &= \frac{1}{2}\overline{u_i' u_i'}, \\ \wp &= -\overline{u_i' u_j'}\frac{\partial U}{\partial x_j}, \\ T &= -\frac{\partial}{\partial x_j}\left(\overline{u_j' p'} + \frac{1}{2}\overline{u_i' u_i' u_j'} - \frac{2}{\mathrm{Re}}\overline{u_i' S_{ij}'}\right), \\ \varepsilon &= -\frac{2}{\mathrm{Re}}\overline{S_{ij}' S_{ij}'}. \end{aligned}$$

An understanding the behavior of turbulent kinetic energy and mechanisms for its production is useful for devising or improving k based turbulence models for tip-leakage flow configurations, and also for investigating the mechanisms for viscous losses in the cascade end-wall region.

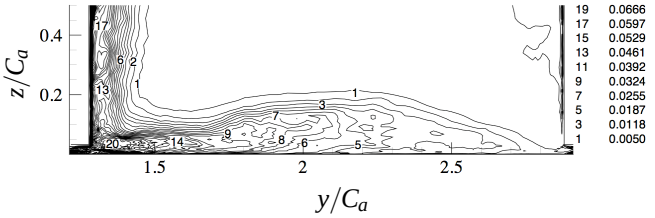

Figure 7. Contour plot of mean turbulent kinetic energy in a $y-z$ plane at $x/C_a = 0.7$.

Figure 7 shows a contour plot of the mean turbulent kinetic energy (k/U_∞^2) at $x/C_a = 0.7$. The gross shape of the turbulent kinetic energy distribution is similar to that found in the mean streamwise velocity contour plot (Fig. 5). The tip-leakage vortex, tip-leakage jet, and blade boundary layer are the main sources of turbulent kinetic energy. More precisely, turbulent kinetic energy found in the tip-leakage jet and blade boundary layer are slightly higher than that in the tip-leakage vortex. Dominance of turbulent kinetic energy in the tip-leakage jet and blade boundary layer region is consistently observed throughout the blade passage. In general, the magnitude of turbulent kinetic energy in the cross-stream plane decreases along the axial direction.

To examine the turbulent kinetic energy production in more detail, each term in $\wp$ (Eq. (1)) is considered separately. The production term is decomposed into:

$$\begin{aligned} \wp = \; & \underbrace{-\overline{u'u'}\frac{\partial U}{\partial x}}_{\approx 0} \quad \underbrace{-\overline{v'v'}\frac{\partial V}{\partial y}}_{\wp_1} \quad \underbrace{-\overline{w'w'}\frac{\partial W}{\partial z}}_{\wp_2} \\ & \underbrace{-\overline{u'v'}\left(\frac{\partial U}{\partial y} + \frac{\partial V}{\partial x}\right)}_{\wp_3} \\ & \underbrace{-\overline{u'w'}\left(\frac{\partial U}{\partial z} + \frac{\partial W}{\partial x}\right)}_{\wp_4} \\ & \underbrace{-\overline{v'w'}\left(\frac{\partial V}{\partial z} + \frac{\partial W}{\partial y}\right)}_{\wp_5}. \end{aligned} \tag{2}$$

Since the first term, $-\overline{u'u'}\frac{\partial U}{\partial x}$, is negligibly small, only the remaining 5 terms are considered.

As shown in Fig. 8, in the cascade passage, the turbulent kinetic energy production near the end wall is dominated by the $\wp_4$ and $\wp_5$ terms. Considering that the magnitudes of Reynolds shear stress components are an order of magnitude smaller than those of Reynolds normal stress components (see Ref. [24]), it is evident that the spanwise derivatives of the mean streamwise and pitchwise velocity components are major sources of turbu-

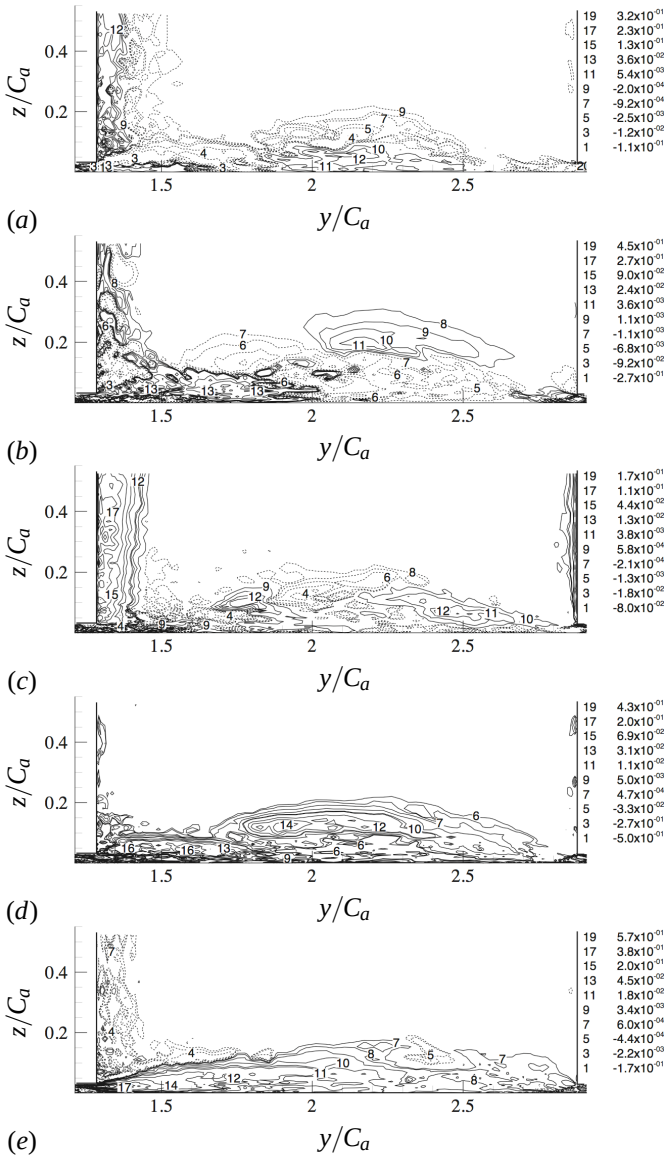

Figure 8. Contour plots of mean turbulent kinetic energy production components in Eq. (2) in a $y-z$ plane at $x/C_a = 0.7$. (*a*) $\wp_1$; (*b*) $\wp_2$; (*c*) $\wp_3$; (*d*) $\wp_4$; (*e*) $\wp_5$.

lent kinetic energy production. The contribution of the $\wp_3$ term to the total $\wp$ is also noticeable due to the pitchwise derivative of the streamwise velocity. The $\wp_3$ term is found to dominate the turbulent kinetic energy production near the blade suction surface. The $\wp_1$ and $\wp_2$ terms are characterized by large regions with opposite signs around the tip-leakage vortex core.

Throughout the blade passage, the tip-leakage jet produces the highest levels of turbulent kinetic energy production. This is due to the large spanwise derivatives of the streamwise or pitchwise velocity components caused by the rapid change of flow direction across the tip gap. Therefore, it is concluded that significant amount of turbulent kinetic energy is produced by the streamwise and pitchwise velocity gradients in the tip-leakage flow. Muthanna and Devenport [15] and Wang and Devenport [16] also reported that most of the turbulence is generated by the axial velocity deficit associated with the tip-leakage vortex rather than its rotating motion.

Considering that the spanwise derivatives of the streamwise and pitchwise velocity components play a major role in producing vorticity and turbulent kinetic energy, it can be inferred that the viscous loss due to the tip-leakage jet can be alleviated by redirecting tip-leakage jet in such a way as to reduce the velocity gradients. Modifications of the blade profile and blade tip may be a feasible way of achieving this. For instance, one may employ a rib like structure to channel the leakage jet towards a desirable direction.

Space-Time Correlations of Velocity Fluctuations

The flow phenomenon associated with viscous losses in the cascade end-wall region is highly turbulent. However, large-scale coherent structures such as the tip-leakage vortex exist in the background turbulent flow and their unsteady characteristics are critically important and yet not well understood.

The unsteady "wandering" motion of the tip-leakage vortex was observed by Zierke *et al.* [13] and others in axial flow rotors. In a recent experiment in a linear cascade employing a stationary end wall, Wenger *et al.* [19] performed two-point correlations of the turbulent fluctuations in the downstream tip-leakage flow, and concluded that the tip-leakage vortex is not subject to low-frequency wandering motions. On the other hand, a subsequent experiment employing a moving end wall [16] showed a low-frequency spectral peak in the pitchwise velocity energy spectra, whose frequency is quite different from the peak frequency in the blade wake. However, no further investigation regarding the origin and mechanism of this low-frequency peak was conducted.

In this study, this issue is examined using the LES data. To examine the spatial and temporal characteristics of the coherent structures present in the tip-leakage flow, energy spectra and space-time correlations of the velocity fluctuations were computed.

Figure 9 shows the energy spectrum of the pitchwise velocity component as a function of frequency at a location in the tip-leakage vortex core. A noticeable spectral peak at non-dimensional frequency of approximately 1.5, which is quite different from the blade wake shedding frequency ($fC/U_\infty = 5 \sim 6$), is observed. The computed spectrum is in excellent agreement with that reported by Wang and Devenport [16]. The same low-frequency peak does not appear in the energy spectra of other velocity components [20].

Considering that the spectral peak appears only in the pitchwise velocity fluctuations, the space-time correlation coefficient

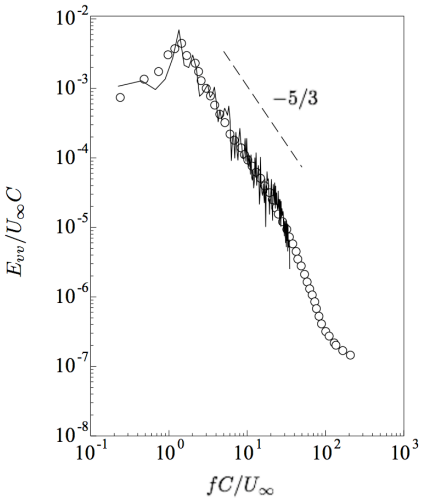

Figure 9. Energy spectra of the pitchwise velocity component as a function of frequency in the tip-leakage vortex core at $x/C_a = 1.51$, $y/C_a = 1.4$, $z/C_a = 0.1$. ——— , LES; ○ , experiment [16]; – – – – , -5/3 slope.

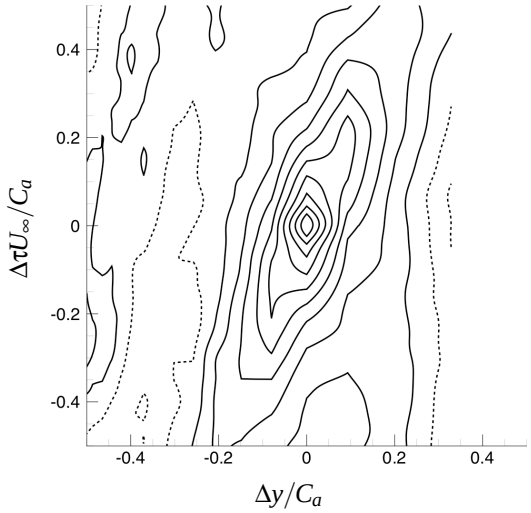

Figure 10. Contour plot of space-time correlations of pitchwise velocity fluctuations as a function of the pitchwise spatial and temporal separations for anchor location at $x/C_a = 1.51$, $y/C_a = 1.4$, $z/C_a = 0.1$. Contours are from -1 to 1 with increments of 0.1.

for each velocity component is computed as a function of pitchwise and temporal separations. Figure 10 shows the space-time correlations of the pitchwise velocity fluctuations at the same location as for Fig. 9. As shown in figure, for small values of pitchwise separation approaches zero, the major axis of the correlation contours is found to be nearly parallel to the time separation axis. This tendency is especially significant for pitchwise velocity fluctuations [24]. This indicates the existence of pitchwise low-frequency wandering motion of the tip-leakage vortex corresponding to the long time delay.

Therefore, the present space-time correlation study suggests that the low-frequency spectral peak observed in the energy spectrum of pitchwise velocity fluctuations is related to the wandering motion of the tip-leakage vortex.

CONCLUSIONS

An analysis of LES results has been performed with an emphasis on understanding the mean flow field, turbulence characteristics, and vortex structures and dynamics in the vicinity and downstream of the tip-gap region.

Gross features of the tip-leakage vortex, tip-separation vortices, and blade wake have been revealed by investigating their evolutionary trajectories and mean velocity fields. The tip-leakage vortex is found to be the most dominant vortical structure in the end-wall region. It is observed to originate on the suction side of the blade tip at about 20% to 30% axial chord downstream from the leading edge. The tip-leakage vortex expands in size and approaches the pressure side of the neighboring blade with increasing axial chord. The trajectory of the tip-leakage vortex in the cascade passage is strongly affected by the moving end wall while the trajectory is mostly influenced by the cascade main stream after passing the trailing edge, where the core of the tip-leakage vortex is sufficiently lifted from the end wall.

In addition, the end-wall vortical structures, including the tip-leakage vortex, are well identified by regions of significant streamwise velocity deficit and high streamwise and pitchwise vorticity magnitudes which suggest a helical configuration. Interestingly, the end-wall region between the blade tip and the tip-leakage vortex produces higher vorticity levels in the streamwise and pitchwise components compared to those in the tip-leakage vortex. This is closely related to the direction of the tip-leakage jet which is generated by the pressure difference between the pressure and suction sides of the blade tip. The tip-leakage jet is found to produce significant spanwise and pitchwise derivatives of the streamwise and pitchwise velocity components which result in highly enhanced vorticity magnitudes.

The tip-leakage vortex, tip-leakage jet, and blade wake are found to generate most of the turbulent kinetic energy. Among them, the tip-leakage jet is found to produce higher levels of the turbulent quantities compared to those generated by the tip-leakage vortex and blade wake throughout the blade passage. This is also due to the large spanwise derivatives of the streamwise or pitchwise velocity components in the tip-leakage jet.

Based on the above analysis, it is expected that the viscous loss due to the tip-leakage jet can be alleviated by changing the direction of the tip-leakage jet such that the spanwise and pitchwise derivatives of the mean velocity are reduced. Modifications

of the blade profile and blade tip may be a feasible way to achieve this. For instance, one may employ a rib like structure to channel the leakage jet towards a desirable direction. A vortex generator which generates vortices rotating in a direction opposite to that of the tip-leakage vortex can also be utilized to diminish its strength.

To examine the spatial and temporal characteristics of the coherent structures present in the tip-leakage flow, space-time correlations of the velocity fluctuations and frequency energy spectra have been computed. The energy spectrum for each velocity component shows broadband characteristics. A notable low-frequency spectral peak is observed in the energy spectrum of the pitchwise velocity fluctuations. A comparison with the vortex shedding frequency in the blade wake and an analysis of the space-time correlations of velocity fluctuations in the endwall tip-leakage flow suggest the existence of a pitchwise wandering motion of the tip-leakage vortex.

ACKNOWLEDGMENT

The authors acknowledge the support of the Office of Naval Research under Grant No. N00014-99-1-0389, with Dr. Ki-Han Kim as program manager. Computer time was provided by a U.S. Department of Defense (DoD) High Performance Computing Modernization Program (HPCMP) Challenge Project Grant (C82) through Army Research Laboratory (ARL) and Aeronautical Systems Center (ASC) Major Shared Resource Centers (MSRC). The authors would also like to thank Professor William Devenport of VPI for providing experimental data and helpful discussions.

REFERENCES

[1] Furukawa, M., Saiki, K., Nagayoshi, K., Kuroumaru, M., and Inoue, M., 1998. "Effects of stream surface inclination on tip leakage flow fields in compressor rotors". *Journal of Turbomachinery,* **120**, pp. 683–694.

[2] Mailach, R., Lehmann, I., and Vogeler, K., 2001. "Rotating instabilities in an axial compressor originating from the fluctuating blade tip vortex". *Journal of Turbomachinery,* **123**, pp. 453–463.

[3] Suder, K. L., 1998. "Blockage development in a transonic, axial compressor rotor". *Journal of Turbomachinery,* **120**, pp. 465–476.

[4] Lakshminarayana, B., and Ravindranath, A., 1982. "Interaction of compressor-rotor blade wake with wall boundary layer/vortex in the end-wall boundary layer". *Journal of Engineering for Power,* **104** (2), April, pp. 467–478.

[5] Lakshminarayana, B., Pouagare, M., and Davino, R., 1982. "Three-dimensional flow-field in the tip region of a compressor rotor passage, part 1: mean velocity profiles and annulus wall boundary layer". *Journal of Engineering for Power,* **104**, October, pp. 760–771.

[6] Pandya, A., and Lakshminarayana, B., 1983. "Investigation of the tip-clearance flow inside and at the exit of a compressor rotor passage. Part 1: mean velocity field". *Journal of Engineering for Power,* **105** (1), pp. 1–12.

[7] Lakshminarayana, B., Sitaram, N., and Zhang, J., 1986. "End-wall and profile losses in a low-speed axial flow compressor rotor". *Journal of Engineering for Gas Turbines and Power,* **108**, pp. 22–31.

[8] Inoue, M., Kuroumaru, M., and Fukuhara, M., 1986. "Behavior of tip-leakage flow behind an axial compressor rotor". *Journal of Engineering for Gas Turbines and Power,* **108**, pp. 7–14.

[9] Goto, A., 1992. "Three-dimensional flow and mixing in an axial flow compressor with different rotor tip clearance". *Journal of Turbomachinery,* **114**, pp. 675–685.

[10] Stauter, R. C., 1993. "Measurements of the three-dimensional tip region flow field in an axial compressor". *Journal of Turbomachinery,* **115**, pp. 468–475.

[11] Lakshminarayana, B., Zaccaria, M., and Marathe, B., 1995. "The structure of tip clearance flow in axial flow compressors". *Journal of Turbomachinery,* **117**, pp. 336–347.

[12] Rains, D. A., 1954. *Tip clearance flows in axial compressors and pumps*. PhD thesis, Division of Engineering and Applied Science, California Institute of Technology, Pasadena, California.

[13] Zierke, W. C., Farrell, K. J., and Straka, W. A., 1995. "Measurement of the tip clearance flow for a high-Reynolds-number axial-flow rotor". *Journal of Turbomachinery,* **117**, pp. 522–532.

[14] Laborde, R., Chantrel, P., and Mory, M., 1997. "Tip clearance and tip vortex cavitation in an axial flow pump". *Journal of Fluids Engineering,* **119**, pp. 680–685.

[15] Muthanna, C., and Devenport, W. J., 2004. "Wake of a compressor cascade with tip gap. Part 1. Mean flow and turbulence structure". *AIAA Journal,* **42** (11), pp. 2320–2331.

[16] Wang, Y., and Devenport, W. J., 2004. "Wake of a compressor cascade with tip gap. Part 2. Effects of endwall motion". *AIAA Journal,* **42** (11), pp. 2332–2340.

[17] Kuhl, D. D., 2001. *Near wall investigation of three dimensional turbulent boundary layers*. Master's thesis, Department of Aerospace and Ocean Engineering, Virginia Polytechnic Institute and State University, Blacksburg, Virginia, August.

[18] Ma, R., 2003. *Unsteady turbulence interaction in a tip leakage flow downstream of a simulated axial compressor rotor*. PhD thesis, Department of Aerospace and Ocean Engineering, Virginia Polytechnic Institute and State University, Blacksburg, Virginia, June.

[19] Wenger, C. W., Devenport, W. J., Wittmer, K. S., and

Muthanna, C., 2004. "Wake of a compressor cascade with tip gap. Part 3. Two-point statistics". *AIAA Journal*, **42** (11), pp. 2341–2346.

[20] You, D., Mittal, R., Wang, M., and Moin, P., 2004. "Computational methodology for large-eddy simulation of tip-clearance flows". *AIAA Journal*, **42** (2), February, pp. 271–279.

[21] Meneveau, C., Lund, T. S., and Cabot, W. H., 1996. "A Lagrangian dynamic subgrid-scale model of turbulence". *Journal of Fluid Mechanics*, **319**, pp. 233–242.

[22] Lund, T. S., Wu, X., and Squires, K. D., 1998. "Generation of turbulent inflow data for spatially-developing boundary layer simulations". *Journal of Computational Physics*, **140**, pp. 233–258.

[23] Fadlun, E. A., Verzicco, R., Orlandi, P., and Mohd-Yusof, J., 2000. "Combined immersed-boundary finite-difference methods for three-dimensional complex flow simulations". *Journal of Computational Physics*, **161**, pp. 35–60.

[24] You, D., Moin, P., Wang, M., and Mittal, R., 2004. *Study of tip clearance flow in a turbomachinery cascade using large eddy simulation*. Report TF-86, Department of Mechanical Engineering, Stanford University, Stanford, California, May.

[25] Akselvoll, K., and Moin, P., 1995. *Large eddy simulation of turbulent confined coannular jets and turbulent flow over a backward facing step*. Report TF-63, Department of Mechanical Engineering, Stanford University, Stanford, California, February.

[26] Jeong, J., and Hussain, F., 1995. "On the identification of a vortex". *Journal of Fluid Mechanics*, **285**, pp. 69–94.